



Species-specific responses of temperate macroalgae with different photosynthetic strategies to ocean acidification: a mesocosm study

Ju-Hyoung Kim¹, Eun Ju Kang², Matthew S. Edwards³, Kitack Lee⁴, Hae Jin Jeong⁵ and Kwang Young Kim^{2,*}

¹Faculty of Marine Applied Biosciences, Kunsan National University, Gunsan 54150, Korea

²Department of Oceanography, Chonnam National University, Gwangju 61186, Korea

³Department of Biology, San Diego State University, 5500 Campanile Drive, Life Sciences North 203, San Diego, CA 92182, USA

⁴School of Environmental Science and Engineering, Pohang University of Science and Technology, Pohang 37673, Korea

⁵School of Earth and Environmental Sciences, College of Natural Sciences, Seoul National University, Seoul 08826, Korea

Concerns about how ocean acidification will impact marine organisms have steadily increased in recent years, but there is a lack of knowledge on the responses of macroalgae. Here, we adopt an outdoor continuous-flowing mesocosm system designed for ocean acidification experiment that allows high CO₂ conditions to vary with natural fluctuations in the environment. Following the establishment of the mesocosm, five species of macroalgae that are common along the coast of Korea (namely *Ulva pertusa*, *Codium fragile*, *Sargassum thunbergii*, *S. horneri*, and *Prionitis cornea*) were exposed to three different CO₂ concentrations: ambient (×1) and elevated CO₂ (2× and 4× ambient), over two-week period, and their ecophysiological traits were measured. Results indicated that both photosynthesis and growth exhibited species-specific responses to the different CO₂ concentrations. Most notably, photosynthesis and growth increased in *S. thunbergii* when exposed to elevated CO₂ conditions but decreased in *P. cornea*. The preference for different inorganic carbon species (CO₂ and HCO₃⁻), which were estimated by gross photosynthesis in the presence and absence of the external carbonic anhydrase (eCA) inhibitor acetazolamide, were also found to vary among species and CO₂ treatments. Specifically, the two *Sargassum* species exhibited decreased eCA inhibition of photosynthesis with increased growth when exposed to high CO₂ conditions. In contrast, growth of *U. pertusa* and *C. fragile* were not notably affected by increased CO₂. Together, these results suggest that the five species of macroalgae may respond differently to changes in ocean acidity, with species-specific responses based on their differentiated photosynthetic acclimation. Understanding these physiological changes might allow us to better predict future changes in macroalgal communities in a more acidic ocean.

Key Words: *Codium fragile*; eCA inhibition; macroalgae; mesocosm; ocean acidification; photosynthesis; *Prionitis cornea*; *Sargassum horneri*; *Sargassum thunbergii*; *Ulva pertusa*



This is an Open Access article distributed under the terms of the Creative Commons Attribution Non-Commercial License (<http://creativecommons.org/licenses/by-nc/3.0/>) which permits unrestricted non-commercial use, distribution, and reproduction in any medium, provided the original work is properly cited.

Received April 29, 2016, Accepted August 20, 2016

*Corresponding Author

E-mail: kykim@chonnam.ac.kr

Tel: +82-62-530-3465, Fax: +82-62-530-0065

INTRODUCTION

Ocean acidification refers to changes in seawater carbon chemistry that result from the increased influx of anthropogenic CO₂ into the oceans (Doney et al. 2009). These changes include decreases in ocean pH, CO₃²⁻ concentrations, and CaCO₃ saturation states, and increases in CO₂ and HCO₃⁻ concentrations. Given that CO₂ and HCO₃⁻ are important in supporting algal photosynthesis and carbon metabolism, many autotrophs will likely be impacted by ocean acidification in both pelagic and coastal ecosystems. Though these impacts are not fully understood, photosynthetic organisms that produce calcium carbonate skeletons will generally be negatively impacted by ocean acidification while non-calcifying macroalgae and seagrasses may be affected variously (Kroeker et al. 2013). Understanding species-specific differences in these impacts, especially for near shore benthic macroalgae, may better allow us to predict how coastal ecosystems will be impacted by further changes in ocean acidity.

Macroalgae are dominant components of rocky shores where even though they occupy only a small area of the coastal region, they account for high percentages of coastal carbon cycles due to their high productivity (Duarte and Cebrián 1996, Mcleod et al. 2011, Kim et al. 2015). Most marine macroalgae photosynthesize using C₃ pathways and are generally able to overcome limited diffusion / supply and poor affinity of CO₂ at the site of CO₂ fixation by taking up HCO₃⁻ from the seawater to use as a carbon source (Giordano et al. 2005, Raven et al. 2008, 2011). This process is facilitated by carbon concentration mechanisms (CCMs), which are strongly associated with the active transport of HCO₃⁻ into the plastid membrane by an enzyme-catalyzed reaction. However, the preferences for different carbon sources that require CCMs are dependent on numerous factors, including the water depth and / or tidal zonation where the macroalgae inhabit (Murru and Sandgren 2004, Hepburn et al. 2011), the total dissolved inorganic carbon (TIC) and / or CO₂ concentrations in the water (Giordano and Maberly 1989, Cornwall et al. 2012, Ní Longphuirt et al. 2013), and the species being considered (Maberly 1990, Maberly et al. 1992). Among these factors, increased seawater CO₂ may be most important to algal photosynthesis and growth, especially in relation to future ocean conditions.

Most macroalgae that have CCMs rely on the enzyme activity of carbonic anhydrase in order to catalyze the conversion from HCO₃⁻ + H⁺ to CO₂ + H₂O, which result in photosynthesis being carbon saturated, or nearly so, at the site of carbon fixation under present ocean condi-

tions (Giordano et al. 2005, Falkenberg et al. 2013). This process, however, requires energy for the biophysical transportation of HCO₃⁻ into the plasma membrane, it might influence the energy cost within the thallus (Raven et al. 2014). Also, the relative composition of different inorganic carbon species in the coastal waters can variously influence carbon saturation states for macroalgal photosynthesis (Gao et al. 2012, Koch et al. 2013). As a result, the metabolic changes required for photosynthetic acclimation to acidified seawater could similarly vary along with the balance between the energy acquisition and consumption, potentially resulting in negative and / or unpredictable physiological responses within the macroalgae. In contrast, species of macroalgae that rely on only a small contribution of CCM for photosynthesis, do not require the same energy to transport HCO₃⁻ into the plasma membrane, but instead rely on ambient CO₂ in the seawater and therefore may respond positively to elevated CO₂ conditions (Raven et al. 2011, Cornwall et al. 2012, Gao et al. 2012, Koch et al. 2013). These species are regularly exposed to, and thus acclimated for, carbon-limited condition suggesting that inorganic carbon needed for photosynthesis is undersaturated under current ocean conditions, and that exposure to chronic CO₂ elevation might result in the enhancement of photosynthesis in them. In this respect, some macroalgae are expected to become more dominant components of their ecosystems under a more acidic ocean while others will decrease in abundance (Hepburn et al. 2011, Johnson et al. 2012). Therefore, understanding the photosynthetic carbon use strategies, combined with knowledge of ocean inorganic carbon saturation states will be integral in predicting ecophysiological and demographic changes in macroalgae under future CO₂ conditions (Cornwall et al. 2012).

Many ocean acidification experiments, to date, have relied on tightly controlled stable laboratory conditions and have focused on single species at a time (Widdicombe et al. 2010). Consequently, the results from stable laboratory experiments do not incorporate natural fluctuations in carbon chemistry or other environmental parameters such as temperature, salinity, and irradiance, and therefore may not adequately reflect true ecological responses expected under elevated CO₂ conditions in the oceans (Cornwall et al. 2013). Thus, field mesocosm experiments may be required if we are to fully interpret the results of these laboratory experiments and apply them to the proper ecological scales in nature (Riebesell et al. 2010). In this study, experiments were conducted within an outdoor continuous-flowing mesocosm system that

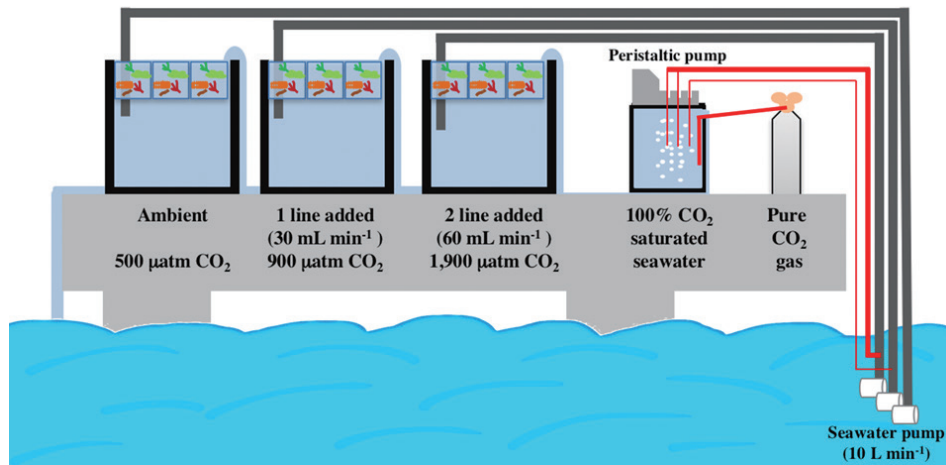


Fig. 1. Schematic of the system used to modify seawater pH and $p\text{CO}_2$ for establishing an outdoor continuous flow-through mesocosm system for ocean acidification research of benthic photosynthetic organisms.

maintained natural variations in seawater CO_2 , temperature, salinity and solar irradiance. The overarching goals of this experiment was to determine how the physiology and ecology of five macroalgae that are dominant components of the Korean coastline are affected by ocean acidification under natural environmental conditions, and to determine the role of external carbonic anhydrase (eCA) in the CCMs of these species. To do this, we traced growth and photosynthetic carbon metabolism in these macroalgae via measurements photosynthesis under ambient and two high CO_2 conditions, and ultimately determined how these were linked to eCA activity.

MATERIALS AND METHODS

CO_2 manipulation and mesocosm system

Our mesocosm system simulated ocean acidification by using multi-channel peristaltic pumps to add CO_2 -saturated seawater into mesocosm inflow pipes, where it

then mixed with ambient seawater to create target pH and CO_2 conditions (Fig. 1). To do this, CO_2 -saturated seawater was prepared by bubbling pure CO_2 gas into seawater within an 80 L tank, decreasing in seawater pH to approximately 5. A peristaltic pump (Masterflex Pump 7523-57; Cole-Parmer Instrument Co., Niles, IL, USA) was then used to inject this water into the mesocosm inflow pipes at different rates to create two elevated CO_2 conditions, with injection rates established by varying the number of injection lines associated with each mesocosm. Ambient seawater (ca. $500 \mu\text{atm CO}_2$) was pumped at a rate of 10 L min^{-1} into the mesocosms using 12-V submersible bilge pumps (capacity: 800 GPH/3,028 LPH; Rule Industries Inc., Burlington, MA, USA), and injection rates of CO_2 -saturated seawater were 30 mL min^{-1} and 60 mL min^{-1} for mesocosms. The seawater CO_2 concentrations were roughly raised to 2 \times ambient (resulting in ca. 0.2 pH unit decrease) and 4 \times ambient (resulting in ca. 0.5 pH unit decrease), respectively (Table 1). Other environmental parameters varied naturally under local conditions. These included natural fluctuations in baseline seawater CO_2

Table 1. Seawater carbon chemistry with adding CO_2 -saturated seawater into natural seawater

	$\text{pH}_{\text{I}}^{\text{(calculated)}}$ Total scale	$A_{\text{T}}^{\text{(measured)}}$ ($\mu\text{mol kg}^{-1}$)	$\text{TIC}^{\text{(measured)}}$ ($\mu\text{mol kg}^{-1}$)	$p\text{CO}_2^{\text{(calculated)}}$ (μatm)	$\text{HCO}_3^-^{\text{(calculated)}}$ ($\mu\text{mol kg}^{-1}$)	$\text{CO}_3^{2-^{\text{(calculated)}}$ ($\mu\text{mol kg}^{-1}$)
$\times 1 \text{ CO}_2$ (ambient)	7.93 ± 0.01	$2,142.48 \pm 4.44$	$1,969.57 \pm 0.85$	505.45 ± 7.97	$1,823.57 \pm 1.34$	128.93 ± 2.35
$\times 2 \text{ CO}_2$ (+30 mL min^{-1})	7.71 ± 0.00	$2,143.42 \pm 1.97$	$2,053.17 \pm 2.11$	902.36 ± 9.06	$1,940.79 \pm 2.30$	81.94 ± 0.83
$\times 4 \text{ CO}_2$ (+60 mL min^{-1})	7.41 ± 0.04	$2,144.41 \pm 4.50$	$2,143.03 \pm 13.47$	$1,867.83 \pm 186.86$	$2,036.20 \pm 11.10$	43.77 ± 4.03

Data are represented as mean \pm standard deviation ($n = 3$).

(484-518 $\mu\text{atm CO}_2$), temperature (20-23°C), salinity (30-32 psu), and daytime integrated irradiance (13.3-25.1 mol photons $\text{m}^{-2} \text{d}^{-1}$). *In situ* nutrient levels in the seawater that was pumped into the mesocosms were $3.09 \pm 0.91 \mu\text{M}$ (nitrite + nitrate), $0.62 \pm 0.30 \mu\text{M}$ (phosphate), and $13.95 \pm 5.54 \mu\text{M}$ (silicate) (data provided by Dr. Jang PG).

The seawater pH (National Bureau of Standards [NBS] scale) within the mesocosms was measured at least five times during each day of the experiment using a pH meter (PHM 210; Radiometer, Copenhagen, Denmark) that was calibrated using the National Institute of Standards and Technology (NIST) standard reference material. The differences in pH among the CO_2 treatments were maintained over the two-week experiment [ambient (control) = 7.95 ± 0.03 ; 2 \times ambient (1 line added) = 7.72 ± 0.06 ; 4 \times ambient (2 lines added) = 7.45 ± 0.15]. In addition, seawater carbon chemistry was measured using potentiometric acid titration as described by Millero et al. (1993). TIC and A_T (total alkalinity) were determined using the methods described in Hernández-Ayón et al. (1999) and Millero et al. (1993), respectively. The CO2sys basic software then used two parameters of the carbonate system (A_T and TIC in this study) to calculate $p\text{CO}_2$ (partial pressure of CO_2), HCO_3^- , and CO_3^{2-} in the seawater (Lewis and Wallace 1998). The precisions of our TIC and A_T estimate were checked with CRMs (certified by A. Dickson, Scripps Institution of Oceanography, San Diego, CA, USA), and were approximately $\pm 5 \mu\text{mol kg}^{-1}$ and $\pm 2 \mu\text{mol kg}^{-1}$, respectively (Kim et al. 2013b).

Sample collection

Five locally abundant species of macroalgae (namely the green algae *Ulva pertusa* and *Codium fragile*, the brown algae *Sargassum horneri* and *S. thunbergii*, and the red alga *Prionitis cornea*) were selected for our experiments. These species are widely distributed on Korean rocky shores, with the relative abundances of *S. thunbergii*, *C. fragile*, and *P. cornea* varying from upper to lower tidal zones. In contrast, *U. pertusa* occurs irrelevant to tidal height (Choi and Kim 2004), while *S. horneri* is commonly distributed subtidal areas where it forms in a forest-like brown alga. Algal samples were collected from 2-5 m water depth near Jangmok on the southern coast of Korea (34.6° N, 128.5° E; South Sea Institute of the KIOST) on Sep 30, 2010, and transported into the mesocosm system described above, which was located adjacent to the sampling site. The macroalgae were immediately placed in approximately 0.5 ton open top outdoor mesocosm tanks (length 120 cm \times width 85 cm \times height 48 cm) equipped

with continuous-flowing ambient seawater for three days to allow the algae to acclimate to the mesocosm environment. Following this, 15 individuals of each species (approximately 0.6 g fresh weight of *U. pertusa*; 2.5 g of *C. fragile*; 1.0 g of *S. horneri*; 2.0 g of *S. thunbergii*; 0.5 g of *P. cornea*) were transferred to mesh plastic cages (length 44 cm \times width 32 cm \times height 20 cm), and three cages were placed into each experimental mesocosm containing the three different CO_2 conditions (ambient, 2 \times ambient, 4 \times ambient). Three plastic cages ($n = 3$) were randomly placed within each mesocosm tank and their positions within the tanks rotated every day. The plastic cages were fixed at the seawater surface and the algae within the cages were mixed frequently to avoid prolonged shading and heterogeneity of water chemistry. The algae were then held within the mesocosms for two weeks in order to examine the impacts of elevated CO_2 on their photosynthesis. All samples chosen for analysis were selected randomly from the three plastic cages and measurements were performed in triplicate.

Photosynthesis (chlorophyll *a* fluorescence and net O_2 production)

Samples were exposed to natural fluctuations in light over the two-week experiment and chlorophyll *a* fluorescence was measured 20 times on each of three individuals at each treatment between dawn and dusk (06:00-20:00 KST), a period that included a wide range of light intensities (0-1,600 $\mu\text{mol photons m}^{-2} \text{s}^{-1}$). Effective quantum yield of PSII (Φ_{PSII}) was measured by *in vivo* chlorophyll *a* fluorescence using a Diving-PAM (Walz, Effeltrich, Germany). The Φ_{PSII} was measured after exposure to *in situ* irradiance condition. A leaf distance clip was equipped on the fiber optic to maintain the light exposed area and distance from the samples surface. The Φ_{PSII} was calculated as $\Phi_{\text{PSII}} = \Delta F/F_m' = (F_m' - F) / F_m'$, where F and F_m' represent the steady-state fluorescence and maximum fluorescence measured in the light, respectively. All Φ_{PSII} measurements were obtained by exposing the samples to a saturation pulse of light followed by different intensities of natural irradiance, and those results represent the apparent efficiency of open PSII reaction centers (Kim et al. 2013a). Relative electron transport rates (rETRs) were calculated as $\text{rETR} = \Phi_{\text{PSII}} \times \text{irradiance}$, and steady-state light response curves (LCs) were constructed as rETR-I curves.

In situ incubation experiments were conducted from dawn to dusk (06:00-20:00 KST) in order to determine steady-state photosynthetic O_2 evolution and consumption rates under natural irradiances, which were mea-

sured using planar oxygen sensor spots (SP-PSt3) and a FIBOX 3 system (PreSens; GmbH, Regensburg, Germany). Working with one individual from each of the five species and three CO₂ treatments (i.e., 15 incubation flasks) at a time, thalli of each macroalga (0.2 g fresh weight of *U. pertusa*, 1.0 g of *C. fragile*, 0.3 g of *S. horneri*, 0.5 g of *S. thunbergii*, and 0.1 g of *P. cornea*) were put into separate 80 mL Corning cell-culture flasks and oxygen concentration was recorded every 30 min under natural light conditions, which was determined to be sufficient time for detecting production and / or consumption of oxygen during photosynthesis and / or respiration. Following this, the algal samples were removed from the flasks, the water replaced, and new 30-min incubations done. Because this resulted in ~30-min time gaps between replicate measurements for each species-CO₂ combination and all photosynthetic measurements were conducted under ambient light conditions, which varied naturally between sample runs, the data for the three macroalgae from each species-CO₂ combination could not be considered replicates and thus photosynthetic parameters could not be represented by their means and standard deviations. Rather, photosynthetic data for the three samples from each treatment combination were represented by independent light response curves, each obtained under a range of irradiances (0-1,500 μmol photons m⁻² s⁻¹), and photosynthetic parameters were calculated for each of the independent P-I (net photosynthesis-irradiance) curves. The three light responses curves for each species-CO₂ combination are represented in electronic supplementary materials (Supplementary Figs S1 & S2). Solar irradiance was recorded using a LI-190 2π PAR sensor connected to a data logger (LI-1400; LI-COR, Lincoln, NE, USA) during the PAM and net photosynthesis measurements and was used to construct the light responses curves, with the data standardized by sample fresh weight (g).

To identify photosynthetic traits, LCs and P-I curves were fitted to a double exponential decay function with a non-linear regression algorithm (Platt et al. 1980). Photosynthetic parameters of LCs (rETR_{m,LC}, maximum relative electron transport rate; α_{LC}, electron transport efficiency; and E_{k,LC}, light-saturation coefficient of LCs) and P-I curves (P_{max}, maximum net photosynthesis rate; α, photosynthetic efficiency; and E_k, irradiance at the onset of light saturation) were determined using the least squares curve fitting technique included with the software Grapher ver. 9.6 (Golden Software Inc., Golden, CO, USA).

Growth rate

The growth rates of the macroalgae were estimated by measuring changes in the fresh wet weights of three replicate fragments of each species after two weeks in the mesocosms; beginning fresh weights were 0.2 g for *U. pertusa*, 1.0 g for *C. fragile*, 0.3 g for *S. horneri*, 0.1 g for *S. thunbergii*, and 0.3 g for *P. cornea*. The specific growth rate (SGR) of each alga was calculated as: SGR (d⁻¹) = ln (W_T / W₀) / (D_T - D₀), where W_T and W₀ represent the sample fresh weights at D_T (after 2 weeks) and D₀ (the initial day), respectively.

Inhibition of eCA

Inhibition of eCA was estimated by gross oxygen production in the presence and absence of the eCA enzyme inhibitor acetazolamide (60 μM of AZ; Sigma-Aldrich, St. Louis, MO, USA) (Israel and Hophy 2002, Kang et al. 2016). To do this, a stock solution of 40 mM AZ was prepared and then diluted 800-fold by adding it to filtered seawater within a ~80 mL water-jacketed respiration chamber. Light was consistently provided to the chambers with intensity of 200 μmol photons m⁻² s⁻¹ by a halogen lamp (KL2500LCD; Schott, Elmsford, NY, USA), and the temperature within the chamber held constant at 22°C. The seawater within the chamber was mixed using a magnetic stirring bar to prevent boundary layer formation. The chamber was then used to measure oxygen production and consumption rates (gross oxygen production) of three replicate samples of each algal species (Kim et al. 2011). Oxygen production was measured using a 2 mm oxygen-dipping probe (DP-PSt3) with a coated foil sensor that was connected to a precise fiber optic oxygen transmitter (FIBOX 3 Oxygen Meter; PreSens GmbH, Regensburg, Germany), and the oxygen changes within the chamber was continuously monitored by personal computer for 20 min under dark and light conditions before and after adding AZ. The eCA inhibition rate of gross photosynthesis (i.e., % of reduced gross photosynthesis by the addition of AZ) was then estimated for each species under each CO₂ treatment.

Statistical analysis

All statistical analyses were performed using SPSS ver. 21 (IBM Corp., Armonk, NY, USA). All data met assumptions of normality and equal variances, as determined by Shapiro-Wilk normality and Levene's homogeneity of variance tests, respectively, except for inhibition rate

of eCA which used AZ. In cases where homogeneity of variances was rejected (inhibition rate of eCA), we used Welch analyses of variance (ANOVA) test to check for consistency among the treatments. Photosynthetic parameters of the LCs and P-I curves, inhibition of eCA activity and growth rates of the macroalgae were each compared among the three CO₂ conditions and five species using separate two-way Model I ANOVAs. Following this, Tukey's *post hoc* multiple comparisons were used to identify specific difference in photosynthetic P-I curve and LCs parameters, and growth among different levels of CO₂ concentrations when the ANOVAs identified those factors to be significant ($p < 0.05$). Paired t tests were used to test

for differences in photosynthesis before versus after adding acetazolamide to the incubation chamber.

RESULTS

Chlorophyll *a* fluorescence and net photosynthetic rate

The five macroalgal species examined in our study exhibited different pattern of rETR-I curves (LCs), but were not noticeably impacted by elevated CO₂ concentrations (Table 2, Supplementary Fig. S1). Further, the LCs did not

Table 2. Photosynthetic parameters of chlorophyll *a* fluorescence (LCs) and net P-I curves of five macroalgal species under the ambient and two ocean acidification conditions ($n = 3$)

Parameter	Species	CO ₂ treatment		
		×1 CO ₂	×2 CO ₂	×4 CO ₂
Chlorophyll <i>a</i> fluorescence parameter				
rETR _{m,LC}	<i>Ulva pertusa</i>	195.47 ± 49.28	156.10 ± 27.95	216.89 ± 63.84
	<i>Codium fragile</i>	479.87 ± 571.82	159.15 ± 74.08	734.90 ± 1075.71
	<i>Sargassum thumbergii</i>	425.78 ± 67.69	471.83 ± 152.41	671.31 ± 527.88
	<i>Sargassum horneri</i>	249.23 ± 34.24	245.19 ± 42.92	257.66 ± 16.58
	<i>Prionitis cornea</i>	864.67 ± 509.51	1,684.85 ± 2,054.68	602.14 ± 404.38
α _{LC}	<i>Ulva pertusa</i>	0.497 ± 0.165	0.702 ± 0.145	0.662 ± 0.291
	<i>Codium fragile</i>	0.354 ± 0.087	0.691 ± 0.236	0.345 ± 0.086
	<i>Sargassum thumbergii</i>	0.945 ± 0.117	0.938 ± 0.353	0.952 ± 0.147
	<i>Sargassum horneri</i>	0.809 ± 0.059	0.839 ± 0.192	0.828 ± 0.214
	<i>Prionitis cornea</i>	0.494 ± 0.025	0.542 ± 0.095	0.663 ± 0.308
E _{k,LC}	<i>Ulva pertusa</i>	433 ± 225	226 ± 40	424 ± 331
	<i>Codium fragile</i>	1,576 ± 2,006	283 ± 236	2,289 ± 3,364
	<i>Sargassum thumbergii</i>	461 ± 131	577 ± 317	779 ± 733
	<i>Sargassum horneri</i>	307 ± 21	306 ± 111	331 ± 118
	<i>Prionitis cornea</i>	1,789 ± 1,150	3,659 ± 4,867	1,177 ± 1,012
Photosynthetic parameter				
P _{max}	<i>Ulva pertusa</i>	326.43 ± 36.27	396.93 ± 113.44	446.69 ± 29.69
	<i>Codium fragile</i>	52.79 ± 18.40	82.19 ± 6.00	71.42 ± 32.51
	<i>Sargassum thumbergii</i>	218.41 ± 100.21	250.89 ± 28.47	329.24 ± 47.61
	<i>Sargassum horneri</i>	368.87 ± 19.77	368.54 ± 95.96	343.67 ± 99.65
	<i>Prionitis cornea</i>	512.72 ± 103.77	497.67 ± 21.19	356.95 ± 52.34
α	<i>Ulva pertusa</i>	2.17 ± 2.35	1.67 ± 0.88	8.81 ± 7.48
	<i>Codium fragile</i>	0.14 ± 0.11	0.35 ± 0.11	0.40 ± 0.18
	<i>Sargassum thumbergii</i>	0.98 ± 1.04	0.80 ± 0.27	1.07 ± 0.28
	<i>Sargassum horneri</i>	0.79 ± 0.05	0.98 ± 0.44	2.60 ± 1.58
	<i>Prionitis cornea</i>	5.62 ± 7.80	2.45 ± 1.49	1.50 ± 0.71
E _k	<i>Ulva pertusa</i>	426 ± 490	265 ± 97	84 ± 66
	<i>Codium fragile</i>	277 ± 156	211 ± 73	135 ± 94
	<i>Sargassum thumbergii</i>	406 ± 261	334 ± 99	315 ± 49
	<i>Sargassum horneri</i>	451 ± 156	439 ± 178	194 ± 55
	<i>Prionitis cornea</i>	352 ± 288	249 ± 115	266 ± 101

LC, steady-state light response curves; P-I, photosynthesis vs. irradiance; rETR_{m,LC}, maximum relative electron transport rate; α_{LC}, electron transport efficiency; E_{k,LC}, light-saturation coefficient of LCs; P_{max}, maximum net photosynthesis rate; α, photosynthetic efficiency; E_k, irradiance at the onset of light saturation.

show inhibition (down-regulation) of photosystem II for any of the macroalgal species under high light intensities. *C. fragile* and *P. cornea*, which exhibited the highest $rETR_{m,LC}$ and $E_{k,LC}$ values, did not reach light saturation under our experimental irradiances. In contrast, *U. pertusa* exhibited the lowest levels of $rETR_{m,LC}$ (195.47 ± 49.28) under ambient conditions. The two *Sargassium* species showed relatively higher α_{LC} than other species (0.945 ± 0.117 for *S. thunbergii* and 0.809 ± 0.059 for *S. horneri*), but there were no significant differences among the other species (Tukey's: $p > 0.05$). The light-saturation coefficients determined by the LCs varied among the macroalgal species under *in situ* light intensities. This indicates that apparent photochemical activity was not impacted by high CO_2 conditions under natural irradiances. Together, photosynthetic parameters of LCs were not significantly impacted by CO_2 and / or macroalgal species except for α_{LC} which varied among the species ($F_{4,30} = 9.426$, $p < 0.001$) (Table 3).

In contrast to LCs, net photosynthetic rates varied slightly among both the macroalgal species and three CO_2 conditions (Table 2, Supplementary Fig. S2). Specifically,

P_{max} varied significantly among the macroalgal species ($F_{4,30} = 48.862$, $p < 0.001$) and interacted with elevated CO_2 ($F_{8,30} = 2.526$, $p = 0.031$), but did not vary among the CO_2 treatment itself ($F_{2,30} = 0.507$, $p > 0.05$) (Table 3). There was no significant individual or combination effects of CO_2 and macroalgal species on the photosynthetic parameters of α and E_k except for macroalgal species for α ($F_{4,30} = 2.768$, $p = 0.045$) and CO_2 for E_k ($F_{2,30} = 3.530$, $p = 0.042$), respectively. Specifically, under ambient conditions, *P. cornea* exhibited the highest P_{max} ($512.72 \pm 103.77 \mu\text{mol O}_2 \text{ g}^{-1} \text{ FW h}^{-1}$), while *C. fragile* exhibited the lowest P_{max} ($52.79 \pm 18.40 \mu\text{mol O}_2 \text{ g}^{-1} \text{ FW h}^{-1}$). Under elevated CO_2 , *U. pertusa* and *S. thunbergii* exhibited obvious enhancement of P_{max} compared to ambient conditions. P_{max} in *U. pertusa* was 21% and 37% and in *S. thunbergii* was 15% and 51% higher under 2 \times and 4 \times ambient CO_2 conditions relative to ambient condition, respectively. In contrast, most noticeable reduced photosynthesis occurred in *P. cornea* (reduced 3% and 30% for P_{max} and 29% and 24% for α under 2 \times and 4 \times ambient CO_2 conditions relative to ambient condition, respectively). Photosynthesis in *S. horneri* did not vary substantially among the CO_2 levels,

Table 3. Analysis of variance examining the effects of CO_2 treatment and macroalgal species on the photosynthetic parameters of LCs and net P-I curves

Parameter	Treatment	Type III sums of squares	Degrees of freedom	Mean squares	F-value	p-value
Chlorophyll <i>a</i> fluorescence parameter						
$rETR_{m,LC}$	CO_2	75,750	2	37,875	0.088	0.916
	Species	4,174,308	4	1,043,576	2.426	0.070
	$CO_2 \times$ Species	2,445,665	8	305,708	0.711	0.680
α_{LC}	CO_2	0.114	2	0.057	1.540	0.231
	Species	1.393	4	0.348	9.426	<0.001***
	$CO_2 \times$ Species	0.239	8	0.030	0.807	0.601
$E_{k,LC}$	CO_2	84,999.743	2	42,410	0.015	0.985
	Species	23,731,273.8	4	5,932,818	2.105	0.105
	$CO_2 \times$ Species	16,386,647.3	8	2,048,331	0.727	0.667
Photosynthetic parameter						
P_{max}	CO_2	4,224	2	2,112	0.507	0.779
	Species	813,898	4	203,474	48.862	<0.001***
	$CO_2 \times$ Species	84,137	8	10,517	2.526	0.031†
α	CO_2	19.913	2	9.957	1.151	0.330
	Species	95.791	4	23.948	2.768	0.045*
	$CO_2 \times$ Species	109.615	8	13.702	1.584	0.171
E_k	CO_2	253,237	2	126,618	3.530	0.042†
	Species	149,794	4	37,448	1.044	0.401
	$CO_2 \times$ Species	110,869	8	13,859	0.386	0.919

LC, steady-state light response curves; P-I, photosynthesis vs. irradiance; $rETR_{m,LC}$, maximum relative electron transport rate; α_{LC} , electron transport efficiency; $E_{k,LC}$, light-saturation coefficient of LCs; P_{max} , maximum net photosynthesis rate; α , photosynthetic efficiency; E_k , irradiance at the onset of light saturation.

* $p < 0.05$, *** $p < 0.001$.

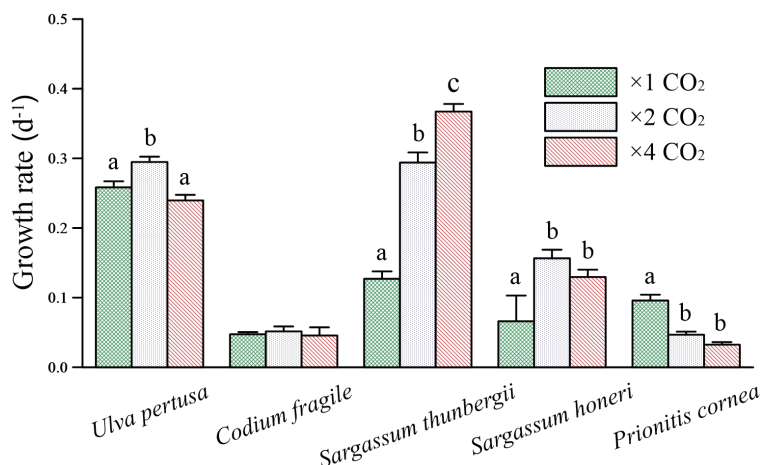


Fig. 2. Mean specific growth rates (μ) of five macroalgal species under the ambient (diagonal cross) and two ocean acidification (dots, 2× ambient; slash, 4× ambient) conditions. Different letters indicate significant differences between treatments at each species based on Tukey’s multiple-comparison ($p < 0.05$). Error bars indicate standard deviation ($n = 3$).

and *C. fragile* exhibited the lowest overall photosynthetic capacity compared with the other species, together making it difficult to distinguish between experimental treatments.

Growth rate

Growth rates varied significantly among the five macroalgal species ($F_{4,30} = 600.846, p < 0.001$) and three CO₂ treatments ($F_{2,30} = 65.986, p < 0.001$) (Table 4, Fig. 2). However, the impact of elevated CO₂ on growth was not consistent among the algal species (Species × CO₂: $F_{8,30} = 68.211, p < 0.001$), indicating that the different species respond differently to elevated CO₂. Specifically, growth in the two species of green algae responded very differently to elevate CO₂, with *U. pertusa* exhibiting the highest growth rates under ambient CO₂ condition and *C. fragile* exhibiting the lowest growth rates. *U. pertusa* growth increased significantly under 2× ambient relative to ambient condition (Tukey’s: $p < 0.01$) but not under 4× ambient condition (Tukey’s: $p > 0.05$), while growth in *C. fragile* remained unaffected by elevated CO₂ (Tukey’s: $p > 0.05$).

Growth in *U. pertusa* increased with elevated CO₂ level (with the maximum observed under 2× ambient conditions), which growth in *C. fragile* remained unaffected by changes in CO₂. Furthermore, growth in both *S. thunbergii* and *S. honeri* increased significantly under 2× ambient CO₂ compared with ambient conditions (Tukey’s: $p < 0.001$ and $p < 0.01$, respectively). In contrast, growth in *S. thunbergii* continued to increase under 4× ambient conditions (Tukey’s: $p > 0.01$) while growth in *S. honeri* remained unchanged relative to 2× ambient conditions (Tukey’s: $p = 0.476$). Growth rate in *P. cornea* decreased significantly under both 2× and 4× ambient relative to ambient condition (Tukey’s: $p > 0.001$), but it did not differ between the two elevated CO₂ treatments (Tukey’s: $p = 0.054$).

Inhibition of eCA

All species exhibited significant reductions in gross photosynthesis after adding the eCA inhibitor (Fig. 3), but differed in the strength of eCA inhibited photosynthesis. Overall, inhibition of eCA activities varied signifi-

Table 4. Analysis of variance examining the effects of CO₂ treatment and macroalgal species on specific growth rate (μ)

	Type III sums of squares	Degrees of freedom	Mean squares	F-value	p-value
CO ₂	0.022	2	0.011	65.986	<0.001***
Species	0.410	4	0.102	600.846	<0.001***
CO ₂ × Species	0.093	8	0.120	68.211	<0.001***

*** $p < 0.001$.

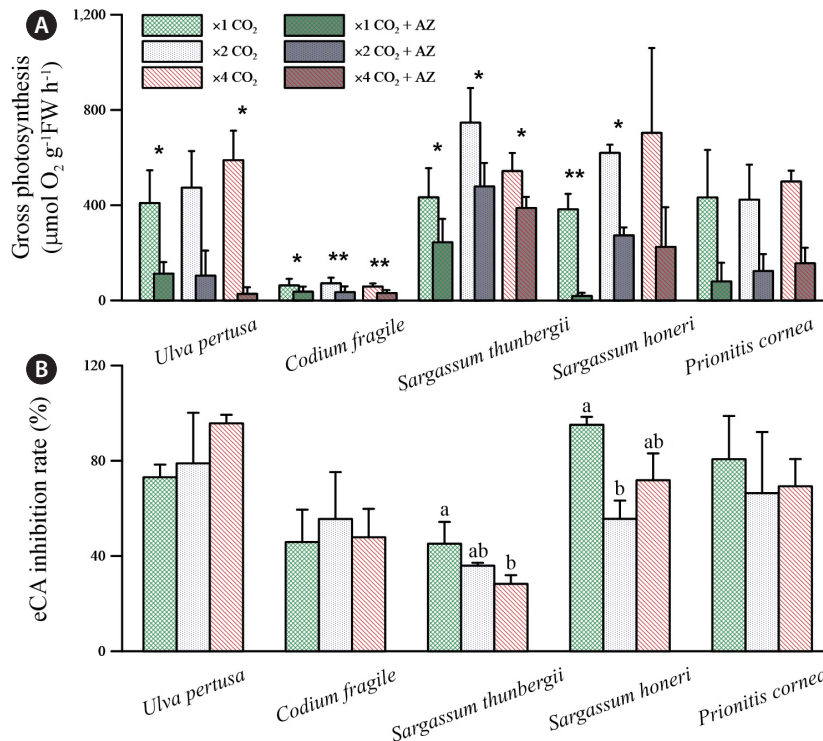


Fig. 3. Effect of external carbonic anhydrase (eCA) inhibitor on gross photosynthesis (A) and eCA inhibition rate on gross photosynthesis (B) under the ambient (diagonal cross) and two ocean acidification (dots, 2 \times ambient; slash, 4 \times ambient) conditions. The data were calculated using gross oxygen production rates in both the presence and absence of the eCA inhibitor (acetazolamide). The asterisk (*) and different letters indicates significant differences between treatments for each species based on paired *t*-test and Tukey's multiple-comparison, respectively (* $p < 0.05$, ** $p < 0.01$). Error bars indicate standard deviation ($n = 3$).

cantly among the five macroalgal species ($F_{4,30} = 18.911$, $p < 0.001$) but not among the three CO₂ concentrations ($F_{2,30} = 1.941$, $p > 0.05$) (Table 5). The relative impact of increased CO₂ concentrations on eCA inhibition also varied significantly among the five macroalgal species ($F_{8,30} = 2.457$, $p < 0.05$). Specifically, *U. pertusa*, *S. horneri*, and *P. cornea* exhibited relatively high inhibition of gross photosynthesis compared with *C. fragile* and *S. thunbergii* when examined under ambient CO₂ conditions, but these results were varied under elevated CO₂ conditions. The photosynthetic rates of *U. pertusa* and *P. cornea* were 490

and 433 $\mu\text{mol O}_2 \text{ g}^{-1} \text{FW h}^{-1}$ when examined under ambient conditions, but decreased 73% and 81%, respectively, after eCA was inhibited (Fig. 3). Although they were not significantly different, eCA inhibition rates in *U. pertusa* increased by 79% and 96% when examined under 2 \times and 4 \times ambient conditions, respectively. *S. horneri* exhibited strong eCA inhibition, with a 95% decrease in its photosynthetic rate following the addition of eCA under ambient conditions, and a 56% and 72% decrease when examined under 2 \times and 4 \times ambient conditions, respectively. *C. fragile* and *S. thunbergii* exhibited roughly a 46%

Table 5. Analysis of variance examining the effects of CO₂ treatment and macroalgal species on inhibition rate of gross photosynthesis (%) after the eCA activity was depressed

	Type III sums of squares	Degrees of freedom	Mean squares	F-value	p-value
CO ₂	679.243	2	339.622	1.941	0.161
Species	13,236.948	4	3,309.237	18.911	<0.001**
CO ₂ \times Species	3,439.098	8	429.887	2.457	0.035*

eCA, external carbonic anhydrase.

* $p < 0.05$, ** $p < 0.01$.

decrease in photosynthesis following the addition of CA, and a lower depression of eCA activity compared to other species under ambient condition. Further, eCA inhibition in *S. thunbergii* was significantly decreased when exposed to high levels of CO₂ relative to ambient condition (Tukey's: $p < 0.05$). In contrast, eCA inhibition in *C. fragile*, *U. pertusa*, and *P. cornea* did not change under elevated CO₂ conditions (Tukey's: $p > 0.05$).

DISCUSSION

Field-based mesocosms have been recognized as ideal tools for evaluating ecological responses by organisms to changes in their environment (Petersen et al. 2009). In contrast, mesocosm systems for studying the impacts of ocean acidification have proven difficult to maintain CO₂ conditions at desired levels while allowing other environmental factors to fluctuate naturally (Havenhand et al. 2010, Widdicombe et al. 2010). For example, several field mesocosm studies have manipulated CO₂ concentrations by bubbling specific CO₂-air gas mixtures into seawater within enclosed mesocosm systems (e.g., Alexandre et al. 2012, Olabarria et al. 2013), but these studies tend to hold CO₂ concentrations constant at these levels and thus do not allow natural daily and / or diurnal variability in CO₂ or other environmental variables. To address this problem, our mesocosm system relies on continuous-flowing seawater with a turnover rate within each tank of less than 45 min, and incorporates natural fluctuations in seawater temperature, salinity, nutrient supply, oxygen and carbon chemistries, and ambient irradiance. We believe this design may be more powerful for studying how macroalgae will respond to future CO₂ levels in the complex coastal environment. However, a limit of this mesocosm study is the small number of mesocosm tanks (replicates) for each CO₂ treatment. First, it is logistically difficult to build and maintain these tanks, and we lack manpower to measure each additional (replicates) tanks. Such problems with pseudoreplication (sensu Hurlbert 1984) have long been recognized as problematic when interpreting the results of ecological studies, and have been particularly prevalent in mesocosm studies where the number of tanks and / or available space is often limited. However, given the efficiency of this system in manipulating CO₂, we believe our mesocosm design is ideal for evaluating impacts of ocean acidification on macroalgal photosynthesis (Havenhand et al. 2010, Widdicombe et al. 2010), but we caution the reader to recognize the lack of replication of mesocosm tanks when applying these results to

the greater coastal zone.

Chlorophyll *a* fluorescences were measured under seminatural conditions, which incorporated daily irradiance cycles. Our results suggest that PSII photochemical performance is not necessarily influenced by variability in CO₂ concentration under conditions of fluctuating light intensities in nature, and it might be hard to detect changes in photochemical activity using seminatural mesocosm studies with acidified seawater. All photo-physiological characteristics were associated with specific times and irradiances, and various responses of photo-physiological changes have been reported for the marine autotrophs (Kim et al. 2013a). For example, changes of chlorophyll *a* fluorescence have been observed under well-controlled laboratory experiments (e.g., pelagic organisms: Fu et al. 2007, Sobrino et al. 2008; and benthic plants: Xu and Gao 2012, Oilschläger and Wiencke 2013) or in mesocosm studies (e.g., Connell and Russell 2010, Olabarria et al. 2013). Results from these studies indicate that some benthic plants do not respond strongly to elevated CO₂ conditions (e.g., Alexandre et al. 2012, Hofmann et al. 2012a, 2012b). However, there are very few studies are aware of where this has been examined under natural outdoor irradiances.

Although chlorophyll *a* fluorescence was not affected by ocean acidification conditions, macroalgal photosynthesis and growth did vary in response to elevated CO₂. Specifically, *U. pertusa* and *S. thunbergii* exhibited increased photosynthetic rates under high CO₂, suggesting that the ambient carbon pool is limited (undersaturated) for photosynthesis. These results may be closely connected with improving photosynthesis in relation to energy allocation (Kim et al. 2013a). From the comparing two of our photosynthesis results (chl *a* fluorescence and net photosynthesis), the energy allocation for photosynthesis between photochemical properties and O₂ production is disproportionate under high CO₂ conditions, a tendency that was already established for pelagic autotrophic organisms (Sobrino et al. 2008, Kim et al. 2013a). In our study, energy utilization efficiency for the photosynthesis was obviously enhanced under high CO₂ in *U. pertusa* and *S. thunbergii*. Additional parameters to determine photosynthetic rates using electron transport rates, which include photorespiration, Mehler reactions and nitrate assimilation, are complicated and highly affected by high CO₂ conditions (Baker and Oxborough 2004). However, *C. fragile* did not respond to changes in CO₂ concentration with respect to photosynthesis (photochemical activity and O₂ production) and growth, because these species are presumably already carbon saturated under ambient

conditions. Consequently, TIC saturation states for photosynthesis in the seawater largely influence the growth of some macroalgal species, but not others. In contrast, *P. cornea* showed decreased net photosynthesis under the highest CO₂ conditions, and it might be that this species is very sensitive to decreases in pH.

Our eCA inhibition results under ambient CO₂ suggest different species of macroalgae have different strategies of carbon acquisition for eCA. In this study, two groups of macroalgae were roughly identified based on their eCA inhibition results under ambient CO₂ conditions; one that describes a highly eCA depressed group (including *U. pertusa*, *S. horneri*, and *P. cornea*), and the other that describes a less eCA sensitive group (including *C. fragile* and *S. thunbergii*). These properties of carbon acquisition under ambient condition are well known from previous physiological studies (e.g., Maberly et al. 1992, Koch et al. 2013) and are in agreement with our results. Also these characteristics could be used to predict how these macroalgal species might acclimate physiologically to elevated CO₂ environments. For example, *S. thunbergii* and *S. horneri* exhibited significantly reduced inhibition of eCA under high CO₂ conditions even though these two species have different carbon acquisition properties under ambient condition, suggesting they could take an advantage of elevated CO₂ by saving energy through the depression of eCA. Consequently, growth rates in the two species of brown algae increased under high CO₂ condition compared to ambient condition. In contrast, three other species examined here, *U. pertusa*, *C. fragile*, and *P. cornea*, did not take advantage of elevated CO₂ with respect to energy cost for eCA modulation. The eCA inhibition rate of *U. pertusa* and *P. cornea* is very high regardless of CO₂ concentration, so their energetic cost remained same or higher than ambient under high CO₂ condition. Growth of *U. pertusa* was not increased under highest CO₂ concentration (4× ambient) even though photosynthesis was enhanced compared to ambient condition owing to energy cost for eCA modulation. All data on photosynthetic and eCA metabolisms seem to be connected to the growth dynamics of marine macroalgae. *P. cornea* was the only exception that did not show changes in eCA inhibition rates, and its photosynthetic rate and growth decreased under the elevated CO₂ conditions. We believe this is most likely due to low pH stress as has been previously observed in other red algae such as *Porphyra linearis* (Israel et al. 1999).

From an ecological perspective, the five macroalgal species have different carbon acquisition strategies that seem to vary along depth and zonation gradients (Hep-

burn et al. 2011). *S. thunbergii* is commonly distributed in the upper subtidal region of our study area where it occasionally experiences exposure to the air where only CO₂ is available as a carbon source (Kim et al. 1998). Forest-like brown algae such as *S. horneri* also experience air exposure that can be unrelated to changes in tidal levels (Golléty et al. 2008), and these species may gain an advantage in their competition with turf algae under high CO₂ conditions (Olabarria et al. 2013). The highest photosynthetic rates among the five species were observed in *S. thunbergii* and were correlated with high tolerance to desiccation during exposure to the atmosphere, with a fast diffusion of atmospheric CO₂ (Ji and Tanaka 2002). Two brown algal species (*S. horneri* and *S. thunbergii*) are frequently exposed to atmospheric CO₂, therefore photosynthetic activity could be stimulated by increased CO₂ through passive CO₂ transport. This tendency is supported by previous studies (e.g., Brown et al. 2014) that report growth of the forest-forming kelp species, *Macrocystis pyrifera*, is significantly stimulated by elevated CO₂ under mesocosm conditions. This also supports the findings of Ní Longphuirt et al. (2013) who demonstrated that some brown algae show significant photosynthetic enhancement when atmospheric CO₂ is increased by a natural occurring CO₂ vent. Specifically, the abundance of brown algae increased significantly near the natural CO₂ vents system, which is also in agreement with our results (Hall-spencer et al. 2008, Johnson et al. 2012).

In contrast to the brown algae, the two green algal species showed little to no responses to the increased CO₂ conditions within our mesocosms. Large amounts of physiological information on the *Ulva* thallus under elevated CO₂ conditions were available from previous studies (e.g., Kang et al. 2016), but there is no comparable result for *C. fragile*. It is generally known that growth of ulvoid species is stimulated under high CO₂ and sufficient N conditions (Gordillo et al. 2001, 2003), but dissolved inorganic nitrogen concentrations were relatively lower than the nitrogen conditions used in previous physiological researches. Obviously, growth of *U. pertusa* was stimulated less than brown algae, and *C. fragile* did not alter their growth under high CO₂ conditions. These two genus act as opportunistic and / or invasive species in coastal areas of temperate region, thus they play an important role in dynamics of macroalgal community fluctuations (Kang et al. 2014, Kang and Kim 2016). If our results represent expressive responses of macroalgae to ocean acidification, blooms of two green algal species could be masked and / or depressed due to over-stimulation of brown algal growth.

In summary, this outdoor flowing-through mesocosm study was conducted to identify the effects of elevated CO₂ on the photosynthetic activities (PSII photochemical activity and O₂ production) and growth metabolisms in marine macroalgae. While previous studies have suggested positive impacts of ocean acidification on metabolic changes in macroalgae, data describing the comparison between photo-physiology and growth metabolism have not been comparatively sufficient. Thus, we investigated physiological responses of five species of macroalgae under different ocean acidification conditions, and our results represent the tracing of this energetic metabolism under high CO₂ conditions. This includes tracing photo-physiological changes associated with the harvesting of light energy to the growth metabolism required for building macroalgal vegetation. Our key finding is that species-specific photosynthetic inorganic saturation states and eCA inhibition are closely related to growth in responses to high CO₂ environments, and these results could be crucial in predicting ecophysiological responses of temperate marine macroalgae in future ocean conditions. In this respect, some macroalgal species can be more positive to CO₂ enhancement than others, resulting in increase of photosynthesis and growth under elevated CO₂ conditions. Based on our results, we suggest that, productivity of *S. thunbergii* might exceed that of *U. pertusa*, resulting in *S. thunbergii* becoming competitively dominant species in this temperate benthic community in the future coastal ocean.

SUPPLEMENTARY MATERIAL

Supplementary Fig. S1. Steady-state light response curves (LCs) of *Ulva pertusa*, *Codium fragile*, *Sargassum thunbergii*, *Sargassum horneri*, and *Prionitis cornea* calculated by effective quantum yield of PSII and *in situ* irradiance under the ambient and two ocean acidification conditions (www.e-algae.org).

Supplementary Fig. S2. Net photosynthesis vs. irradiance (P-I) curves of *Ulva pertusa*, *Codium fragile*, *Sargassum thunbergii*, *Sargassum horneri*, and *Prionitis cornea* under the ambient and two ocean acidification conditions (www.e-algae.org).

ACKNOWLEDGEMENTS

We thank Dr. Shin K, Dr. Jang PG, Dr. Jang MC, and Dr. Hyun B for field assistance, and Dr. Park K, and Dr.

Kim H-C for technical suggestions on the mesocosm experiment. This work was supported by the program on “Management of Marine Organisms causing Ecological Disturbance and Harmful Effects” funded by KIMST/MOF and NRF-2016R1A6A1A03012647 to KYK, and NRF-2015R1C1A1A01054831 to JHK.

REFERENCES

- Alexandre, A., Silva, J., Buapet, P., Björk, M. & Santos, R. 2012. Effects of CO₂ enrichment on photosynthesis, growth, and nitrogen metabolism of the seagrass *Zostera noltii*. *Ecol. Evol.* 2:2625-2635.
- Baker, N. R. & Oxborough, K. 2004. Chlorophyll fluorescence as a probe of photosynthetic productivity. In Papa-georgiou, G. C. & Govindjee (Eds.) *Chlorophyll a Fluorescence: A Signature of Photosynthesis*. Springer, Dordrecht, pp. 65-82.
- Brown, M. B., Edwards, M. S. & Kim, K. Y. 2014. Effects of climate change on the physiology of giant kelp, *Macrocystis pyrifera*, and grazing by purple urchin, *Strongylocentrotus purpuratus*. *Algae* 29:203-215.
- Choi, T. S. & Kim, K. Y. 2004. Spatial pattern of intertidal macroalgal assemblages associated with tidal levels. *Hydrobiologia* 512:49-56.
- Connell, S. D. & Russell, B. D. 2010. The direct effects of increasing CO₂ and temperature on non-calcifying organisms: increasing the potential for phase shifts in kelp forests. *Proc. Biol. Sci.* 277:1409-1415.
- Cornwall, C. E., Hepburn, C. D., McGraw, C. M., Currie, K. I., Pilditch, C. A., Hunter, K. A., Boyd, P. W. & Hurd, C. L. 2013. Diurnal fluctuations in seawater pH influence the response of a calcifying macroalga to ocean acidification. *Proc. Biol. Sci.* 280:20132201.
- Cornwall, C. E., Hepburn, C. D., Pritchard, D., Currie, K. I., McGraw, C. M., Hunter, K. A. & Hurd, C. L. 2012. Carbon-use strategies in macroalgae: differential responses to lowered pH and implications for ocean acidification. *J. Phycol.* 48:137-144.
- Doney, S. C., Fabry, V. J., Feely, R. A. & Kleypas, J. A. 2009. Ocean acidification: the other CO₂ problem. *Annu. Rev. Mar. Sci.* 1:169-192.
- Duarte, C. M. & Cebrián, J. 1996. The fate of marine autotrophic production. *Limnol. Oceanogr.* 41:1758-1766.
- Falkenberg, L. J., Russell, B. D. & Connell, S. D. 2013. Contrasting resource limitations of marine primary producers: implications for competitive interactions under enriched CO₂ and nutrient regimes. *Oecologia* 172:575-583.

- Fu, F. -X., Warner, M. E., Zhang, Y., Feng, Y. & Hutchins, D. A. 2007. Effects of increased temperature and CO₂ on photosynthesis, growth, and elemental ratios in marine *Synechococcus* and *Prochlorococcus* (Cyanobacteria). *J. Phycol.* 43:485-496.
- Gao, K., Helbling, E. W., Häder, D. -P. & Hutchins, D. A. 2012. Responses of marine primary producers to interactions between ocean acidification, solar radiation, and warming. *Mar. Ecol. Prog. Ser.* 470:169-189.
- Giordano, M., Beardall, J. & Raven, J. A. 2005. CO₂ concentrating mechanisms in algae: mechanisms, environmental modulation, and evolution. *Annu. Rev. Plant Biol.* 56:99-131.
- Giordano, M. & Maberly, S. C. 1989. Distribution of carbonic anhydrase in British marine macroalgae. *Oecologia* 81:534-539.
- Golléty, C., Migné, A. & Davoult, D. 2008. Benthic metabolism on a sheltered rocky shore: role of the canopy in the carbon budget. *J. Phycol.* 44:1146-1153.
- Gordillo, F. J. L., Figueroa, F. L. & Niell, F. X. 2003. Photon- and carbon-use efficiency in *Ulva rigida* at different CO₂ and N levels. *Planta* 218:315-322.
- Gordillo, F. J. L., Niell, F. X. & Figueroa, F. L. 2001. Non-photosynthetic enhancement of growth by high CO₂ level in the nitrophilic seaweed *Ulva rigida* C. Agardh (Chlorophyta). *Planta* 213:64-70.
- Hall-spencer, J. M., Rodolfo-Metalpa, R., Martin, S., Ransome, E., Fine, M., Turner, S. M., Rowley, S. J., Tedesco, D. & Buia, M. -C. 2008. Volcanic carbon dioxide vents show ecosystem effects of ocean acidification. *Nature* 454:96-99.
- Havenhand, J., Dupont, S. & Quinn, G. P. 2010. Designing ocean acidification experiments to maximize inference. In Riebesell, U., Fabry, V. J., Hansson, L. & Gattuso, J. -P. (Eds.) *Guide to Best Practices in Ocean Acidification Research and Data Reporting*. Publications Office of the European Union, Luxembourg, pp. 67-80.
- Hepburn, C. D., Pritchard, D. W., Cornwall, C. E., McLeod, R. J., Beardall, J., Raven, J. A. & Hurd, C. L. 2011. Diversity of carbon use strategies in a kelp forest community: implications for a high CO₂ ocean. *Glob. Chang. Biol.* 17:2488-2497.
- Hernández-Ayón, J. M., Belli, S. L. & Zirino, A. 1999. pH, alkalinity and total CO₂ in coastal seawater by potentiometric titration with a difference derivative readout. *Anal. Chim. Acta* 394:101-108.
- Hofmann, L. C., Straub, S. & Bischof, K. 2012a. Competition between calcifying and noncalcifying temperate marine macroalgae under elevated CO₂ levels. *Mar. Ecol. Prog. Ser.* 464:89-105.
- Hofmann, L. C., Yildiz, G., Hanelt, D. & Bischof, K. 2012b. Physiological responses of the calcifying rhodophyte, *Corallina officinalis* (L.), to future CO₂ levels. *Mar. Biol.* 159:783-792.
- Hurlbert, S. H. 1984. Pseudoreplication and the design of ecological field experiments. *Ecol. Monogr.* 54:187-211.
- Israel, A. & Hophy, M. 2002. Growth, photosynthetic properties and Rubisco activities and amounts of marine macroalgae grown under current and elevated seawater CO₂ concentrations. *Glob. Chang. Biol.* 8:831-840.
- Israel, A., Katz, S., Dubinsky, Z., Merrill, J. E. & Friedlander, M. 1999. Photosynthetic inorganic carbon utilization and growth of *Porphyra linearis* (Rhodophyta). *J. Appl. Phycol.* 11:447-453.
- Ji, Y. & Tanaka, J. 2002. Effect of desiccation on the photosynthesis of seaweeds from the intertidal zone in Honshu, Japan. *Phycol. Res.* 50:145-153.
- Johnson, V. R., Russell, B. D., Fabricius, K. E., Brownlee, C. & Hall-Spencer, J. M. 2012. Temperate and tropical brown macroalgae thrive, despite decalcification, along natural CO₂ gradients. *Glob. Chang. Biol.* 18:2792-2803.
- Kang, E. J., Kim, J. -H., Kim, K., Choi, H. -G. & Kim, K. Y. 2014. Re-evaluation of green tide-forming species in the Yellow Sea. *Algae* 29:267-277.
- Kang, E. J., Kim, J. -H., Kim, K. & Kim, K. Y. 2016. Adaptations of a green tide forming *Ulva linza* (Ulvophyceae, Chlorophyta) to selected salinity and nutrients conditions mimicking representative environments in the Yellow Sea. *Phycologia* 55:210-218.
- Kang, E. J. & Kim, K. Y. 2016. Effects of future climate conditions on photosynthesis and biochemical component of *Ulva pertusa* (Chlorophyta). *Algae* 31:49-59.
- Kim, J. -H., Kang, E. J., Kim, K., Jeong, H. J., Lee, K., Edwards, M. S., Park, M. G., Lee, B. -G. & Kim, K. Y. 2015. Evaluation of carbon flux in vegetative bay based on ecosystem production and CO₂ exchange driven by coastal autotrophs. *Algae* 30:121-137.
- Kim, J. -H., Kang, E. J., Park, M. G., Lee, B. -G. & Kim, K. Y. 2011. Effects of temperature and irradiance on photosynthesis and growth of a green-tide-forming species (*Ulva linza*) in the Yellow Sea. *J. Appl. Phycol.* 23:421-432.
- Kim, J. -H., Kim, K. Y., Kang, E. J., Lee, K., Kim, J. -M., Park, K. -T., Shin, K., Hyun, B. & Jeong, H. J. 2013a. Enhancement of photosynthetic carbon assimilation efficiency by phytoplankton in the future coastal ocean. *Biogeosciences* 10:7525-7535.
- Kim, J. -H., Lam, S. M. N. & Kim, K. Y. 2013b. Photoacclimation strategies of the temperate coralline alga *Corallina officinalis*: a perspective on photosynthesis, calcification, photosynthetic pigment contents and growth. *Al-*

- gae 28:355-363.
- Kim, K. Y., Choi, T. S., Huh, S. H. & Garbary, D. J. 1998. Seasonality and community structure of subtidal benthic algae from Daedo Island, Southern Korea. *Bot. Mar.* 41:357-365.
- Koch, M., Bowes, G., Ross, C. & Zhang, X. -H. 2013. Climate change and ocean acidification effects on seagrasses and marine macroalgae. *Glob. Chang. Biol.* 19:103-132.
- Kroeker, K. J., Kordas, R. L., Crim, R., Hendriks, I. E., Ramajo, L., Singh, G. S., Duarte, C. M. & Gattuso, J. -P. 2013. Impacts of ocean acidification on marine organisms: quantifying sensitivities and interaction with warming. *Glob. Chang. Biol.* 19:1884-1896.
- Lewis, E. & Wallace, D. W. R. 1998. *Program developed for CO₂ system calculation*. ORNL/CDIAC-105. Carbon Dioxide Information Analysis Center. Oak Ridge National Laboratory, U.S. Department of Energy, Oak Ridge, TN, 33 pp.
- Maberly, S. C. 1990. Exogenous sources of inorganic carbon for photosynthesis by marine macroalgae. *J. Phycol.* 26:439-449.
- Maberly, S. C., Raven, J. A. & Johnston, A. M. 1992. Discrimination between ¹²C and ¹³C by marine plants. *Oecologia* 91:481-492.
- McLeod, E., Chmura, G. L., Bouillon, S., Salm, R., Björk, M., Duarte, C. M., Lovelock, C. E., Schlesinger, W. H. & Silliman, B. R. 2011. A blueprint for blue carbon: toward an improved understanding of the role of vegetated coastal habitats in sequestering CO₂. *Front. Ecol. Environ.* 9:552-560.
- Millero, F. J., Zhang, J. -Z., Lee, K. & Campbell, D. M. 1993. Titration alkalinity of seawater. *Mar. Chem.* 44:153-165.
- Murru, M. & Sandgren, C. D. 2004. Habitat matters for inorganic carbon acquisition in 38 species of red macroalgae (Rhodophyta) from Puget Sound, Washington, USA. *J. Phycol.* 40:837-845.
- Ní Longphuirt, S., Eschmann, C., Russell, C. & Stengel, D. B. 2013. Seasonal and species-specific response of five brown macroalgae to high atmospheric CO₂. *Mar. Ecol. Prog. Ser.* 493:91-102.
- Oilschläger, M. & Wiencke, C. 2013. Ocean acidification alleviates low-temperature effects on growth and photosynthesis of the red alga *Neosiphonia harveyi* (Rhodophyta). *J. Exp. Bot.* 64:5587-5597.
- Olabarria, C., Arenas, F., Viejo, R. M., Gestoso, I., Vaz-Pinto, F., Incera, M., Rubal, M., Cacabelos, E., Veiga, P. & Sobrino, C. 2013. Response of macroalgal assemblages from rockpools to climate changes: effects of persistent increase in temperature and CO₂. *Oikos* 122:1065-1079.
- Petersen, J. E., Kennedy, V. S., Dennison, W. C. & Kemp, W. M. 2009. *Enclosed experimental ecosystem and scale: tools for understanding and managing coastal ecosystem*. Springer, New York, 222 pp.
- Platt, T., Gallegos, C. L. & Harrison, W. G. 1980. Photoinhibition of photosynthesis in natural assemblages of marine phytoplankton. *J. Mar. Res.* 38:687-701.
- Raven, J. A., Beardall, J. & Giordano, M. 2014. Energy costs of carbon dioxide concentrating mechanisms in aquatic organisms. *Photosynth. Res.* 121:111-124.
- Raven, J. A., Cockell, C. S. & De La Rocha, C. L. 2008. The evolution of inorganic carbon concentrating mechanisms in photosynthesis. *Philos. Trans. R. Soc. Lond. B Biol. Sci.* 363:2641-2650.
- Raven, J. A., Giordano, M., Beardall, J. & Marberly, S. C. 2011. Algal and aquatic plant carbon concentrating mechanisms in relation to environmental change. *Photosynth. Res.* 109:281-296.
- Riebesell, U., Lee, K. & Nejtgaard, J. C. 2010. Pelagic mesocosms. In Riebesell, U., Fabry, V. J., Hansson, L. & Gattuso, J. -P. (Eds.) *Guide to Best Practices in Ocean Acidification Research and Data Reporting*. Publications Office of the European Union, Luxembourg, pp. 81-98.
- Sobrino, C., Ward, M. L. & Neale, P. J. 2008. Acclimation to elevated carbon dioxide and ultraviolet radiation in the diatom *Thalassiosira pseudonana*: effects on growth, photosynthesis, and spectral sensitivity of photoinhibition. *Limnol. Oceanogr.* 53:494-505.
- Widdicombe, S., Dupont, S. & Thorndyke, M. 2010. Laboratory experiments and benthic mesocosm studies. In Riebesell, U., Fabry, V. J., Hansson, L. & Gattuso, J. -P. (Eds.) *Guide to Best Practices in Ocean Acidification Research and Data Reporting*. Publications Office of the European Union, Luxembourg, pp. 113-122.
- Xu, J. & Gao, K. 2012. Future CO₂-induced ocean acidification mediates the physiological performance of a green tide alga. *Plant Physiol.* 160:1762-1769.